2022

Frequency Distribution Control for Flow-induced Noise Mitigation Near Expansion Device

Yingyue Zhang

Stefan Elbel

Frequency distribution control for flow-induced noise mitigation near expansion device

Yingyue ZHANG[1]*, Stefan ELBEL[2]*

[1] Air Conditioning and Refrigeration Center
Department of Mechanical Science and Engineering
University of Illinois at Urbana-Champaign
1206 West Green Street, Urbana, IL, 61801, USA
Phone: +1 (217) 819-8603; Email: yingyue2@illinois.edu

[2] Creative Thermal Solutions, Inc.,
2209 North Willow Road, Urbana, IL 61802, USA
Phone: +1 (217) 244-1531; Email: elbel@illinois.edu

* Corresponding Author

ABSTRACT

Flow-induced noise near the expansion devices can be very annoying to the nearby occupants. Current studies related to flow-induced noise mitigation are focused on the control of noise amplitude. Also, the mitigation of flow-induced noise usually requires extra installation space. In this paper, a new flow-induced noise mitigation method is introduced. Stainless steel mesh is used to modify flow regimes and noise frequency distribution. The mesh can help the bubbles break into smaller ones, thus controlling the frequency of bubbles. A pump R134a system is tested with a needle valve installed in the semi-anechoic chamber. The mitigation effects of flow-induced noise are compared with mesh installed in different sizes and positions. The results show that when the mesh is installed at the valve's outlet, the mitigation effect is better than installed at the inlet. The best mitigation effect shows up when the mesh size is 75 microns. With the help of a high-speed camera, the variation of flow regimes is displayed in this paper. Since the mesh accelerates the flow near the expansion devices, the mitigation of flow-induced noise is also related to the mass flux of flow after acceleration. Also, it shows that noise mitigation decreases as the installation position is further to the valve body.

1. INTRODUCTION

Flowing-induced noise near the expansion devices can be very disturbing, and the mitigation of flow-induced noise becomes more and more important. The flow-induced noise is caused by the vapor flow at the expansion device inlet. Also, the flow regimes before entering the expansion device also influence the annoyance of flow-induced noise. In the current studies related to flow-induced noise mitigation, reducing the amplitude of flow-induced noise is usually the focus. Han *et al.* (2010) modified the shape of the evaporator inlet tube to control the inlet flow regimes of the evaporator. However, the method is limited by the position of other components in the system. The modification of system design can be very costly. Wang *et al.* (2016) studied the coalescence of liquid droplets. Kim and Song (2020) showed the mitigation results of flow-induced noise by using porous material and honeycomb near the expansion device. An extra cylinder is made to install the porous material and honeycomb near the expansion device. The porous material and honeycomb installation occupy extra space, which is not very feasible for an HVAC system.

Therefore, the authors would like to introduce another method to mitigate flow-induced noise in this study. Instead of controlling the amplitude of flow-induced noise, the paper discusses controlling the frequency of flow-induced noise. The frequency distribution is controlled by using the stainless-steel mesh near the expansion devices. Also, mesh installation does not occupy extra space in the system, which is more applicable to industrial systems.

2. METHODOLOGY

2.1 Psychoacoustic annoyance

A sound evaluation parameter called psychoacoustic annoyance is used in the paper. Psychoacoustic annoyance is a

comprehensive parameter that can describe the noise frequency and amplitude simultaneously. The parameter is defined based on investigating people's feelings about different types of noise.

In the psychoacoustic noise evaluation system, the parameter used to evaluate the sound's amplitude is called loudness. Loudness is a subjective perception of sound pressure. By dividing the sensitive human audible frequency range (20 Hz and 15.5 kHz) into 24 barks, the definition of loudness is defined in equation 1 (Fastl and Zwicker, 1999):

$$\mathrm{L} = \int_0^{24\mathrm{Bark}} \mathrm{N}'(\mathrm{k})\mathrm{dk} \tag{1}$$

The sound pressure level describes the amplitude of sound at a certain frequency, while the loudness describes the overall subjective perception of flow-induced noise within a period. The relationship between the average sound pressure level and the loudness within a period is given in equation 2:

$$\mathrm{SPL} = 30 + 33.2\log 10(\mathrm{L}) \tag{2}$$

In the psychoacoustic noise evaluation system, the parameter used to evaluate sound frequency is called sharpness. Higher sharpness indicates a larger proportion of high-frequency noise. The definition of sharpness is given in equation 3 and equation 4 (Fastl and Zwicker, 1999):

$$\mathrm{S} = 0.11 \frac{\int_0^{24\mathrm{Bark}} \mathrm{N}'(\mathrm{k})\mathrm{g}\prime(\mathrm{k})\mathrm{k}\,\mathrm{dk}}{\int_0^{24\mathrm{Bark}} \mathrm{N}'(\mathrm{k})\mathrm{dk}} \tag{3}$$

$$\begin{cases} \mathrm{k} < 14 & \mathrm{g}'(\mathrm{k}) = 1 \\ \mathrm{k} > 14 & \mathrm{g}'(\mathrm{k}) = 0.00012\mathrm{k}^4 - 0.0056\mathrm{k}^3 + 0.1\mathrm{k}^2 - 0.81\mathrm{k} + 3.51 \end{cases} \tag{4}$$

Roughness and fluctuation strength quantify the subjective perception of flow-induced noise related to modulation. Therefore, the paper does not consider roughness terms and fluctuation strength terms. The expression of psychoacoustic annoyance can be simplified in equation 5 and equation 6 (Fastl and Zwicker, 1999):

$$\mathrm{PA} = \mathrm{N}_5(1 + \mathrm{w}_{\mathrm{SL}}) \tag{5}$$

$$\begin{cases} \mathrm{w}_{\mathrm{SL}} = (\mathrm{S} - 1.75)\, 0.25\log(\mathrm{N}_5 + 10) & \mathrm{S} > 1.75 \\ 0 & \mathrm{S} < 1.75 \end{cases} \tag{6}$$

Where N_5 represents that loudness value that exceeds 95% of the noise loudness within measuring time.

2.2 Frequency of bubble oscillation frequency

The oscillation frequency of bubbles is determined by bubble radius and the local pressure. The oscillation of bubbles causes the pressure variation of the flow. The pressure variation of the flow is the main source of flow-induced noise. For one thing, bubbles and droplets are generated during the throttling process. In addition, many cavitation bubbles appear downstream because of the sudden pressure change. The existence of bubbles near the expansion devices causes high-frequency flow-induced noise. The natural frequency of a spherical bubble is given by equation 7 (Minnaert, 1933):

$$\mathrm{f}_{\mathrm{na}} = \frac{1}{2\pi \mathrm{r}_{\mathrm{eq}}} \sqrt{\frac{3\mathrm{YP}_{\mathrm{l}}}{\rho_{\mathrm{l}}}} \tag{7}$$

In this paper, the polytropic exponent is set as 1.4.

The frequency of bubble oscillations can be controlled by changing the size of bubbles. When the bubble size is smaller than 0.5mm, the frequency of bubble oscillation exceeds the human audible zone so that it cannot be heard. In this case, the external structure, such as the steel stainless mesh, can be used to control the size of bubbles. When the bubbles and droplets pass through the mesh, bubbles are broken into smaller ones. In this case, the oscillation frequency of bubbles increases.

3. EXPERIMENTAL SETUP

This paper uses a needle valve as the expansion device in a pumped R134a loop. First, the stainless-steel mesh is installed near the expansion device, as shown in Figure 1. In Figure 1, the mesh is cut into a circle shape with the same diameter as the tube diameter. The mesh can be fixed near the expansion devices by connecting the tubes with the needle valve. Both the straight valve and the angle valve are used for testing. The straight valve is SS-1RS6, and the angle valve is SS-1RS6-A. In this case, the internal structure for the needle valve and the angle valve is the same. In this paper, the mesh size varies from 25um to 200um. The structure of the 25um mesh is shown as an example in Figure 1.

Figure 2(a) shows a system schematic of the pumped R134a system. The test section is placed inside the anechoic chamber, and a microphone is used for the noise measurement. The sampling rate of the microphone is set to 44.2 kHz. The human audible zone is from 20 Hz to 20 kHz. The spectra's frequency range is half the sampling rate after transferring the noise signal from the time domain to the spectra domain. In Figure 2(b), a high-speed camera is used to visualize the flow regimes before and after passing through the mesh. The design is shown in Figure 2(c) when locating the mesh in the transparent PFA tube. Two ¼-inch tube is inserted into a 3/8-inch tube, the total length of which is the same as the 3/8-inch tube—installing the round mesh with a 3/8-inch diameter at the designed position by adjusting the length of the two ¼ inch tube. This design can simultaneously visualize the flow regimes before and after passing through the mesh.

There are a total of 5 thermocouples, 2 pressure transducers, and one mass flow meter in this setup. The quality of inlet R134a flow varies from 0 to 0.6. The pressure difference between the inlet and outlet is 250 kPa, and the mass flux is about 250 kg/ms^2. A summary of the uncertainty analysis is shown in Table 1.

Table 1. Summary of measured and calculated property uncertainties

Thermocouple reading (°C)	Mass flow rate reading (g/s)	Pressure reading (kPa)	Quality (–)
±0.5	±0.1	±7	±0.06

(a)

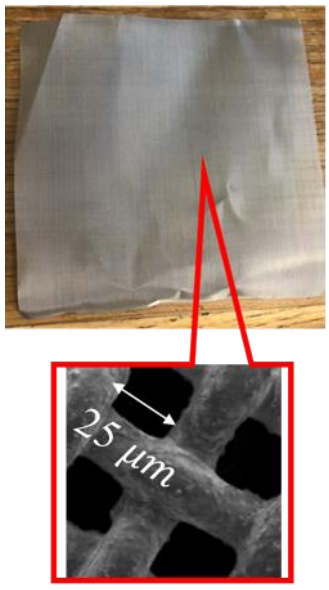

(b)

Angle valve

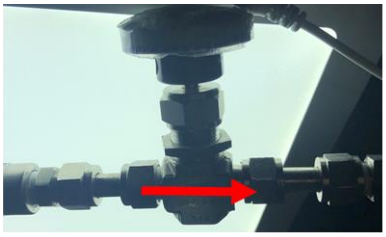

Straight valve

(c)

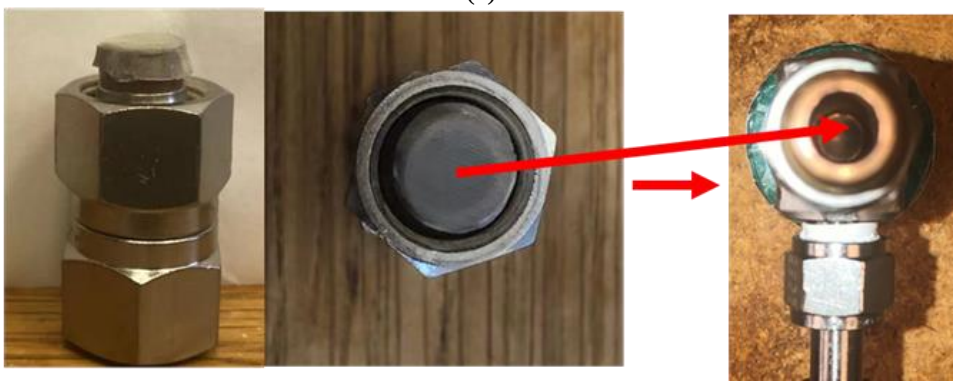

Figure 1. The installation of stainless-steel mesh (a) structure of stainless-steel mesh with 25um mesh size (b) type of expansion valves (c) position of mesh installation

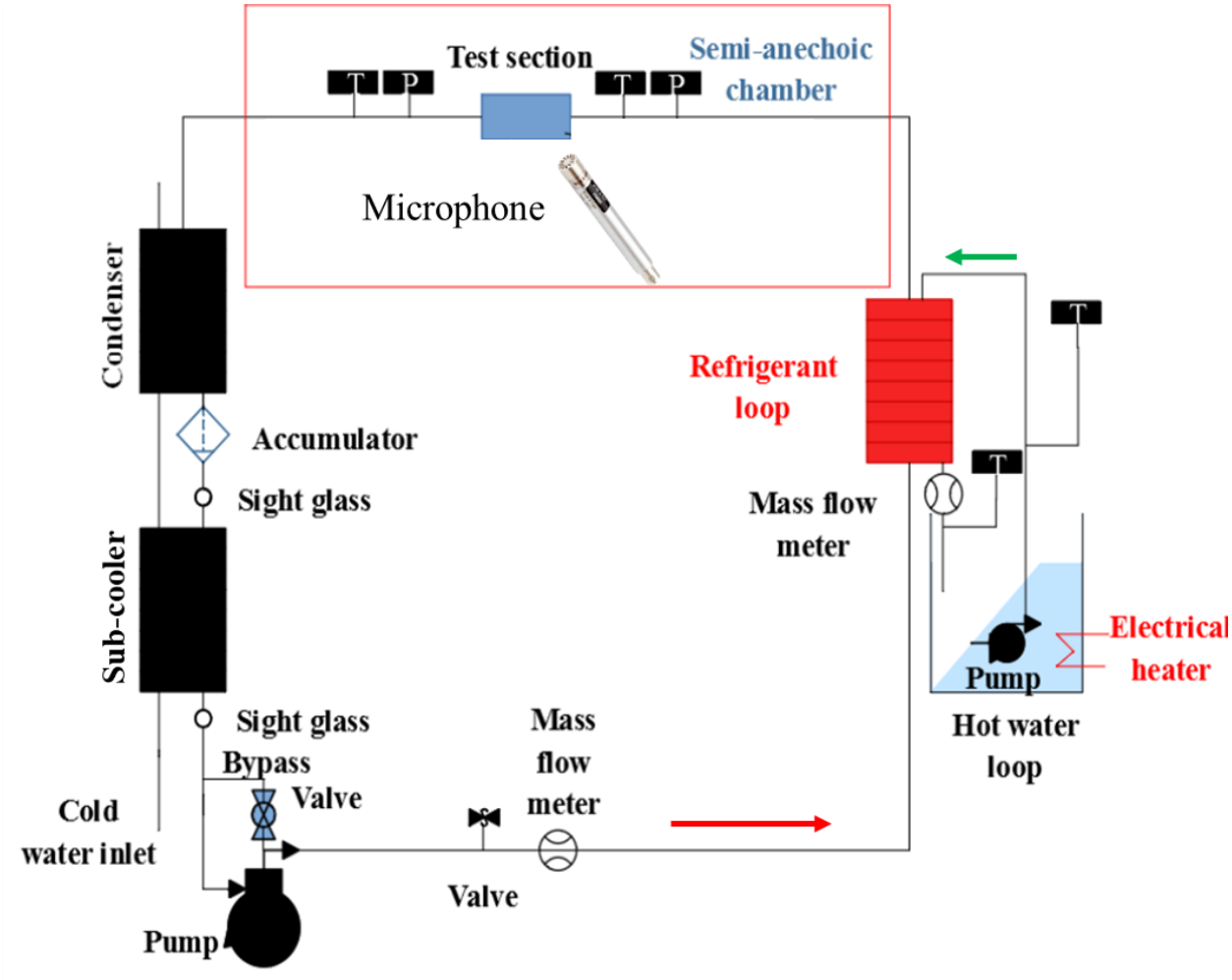

(b) (c)

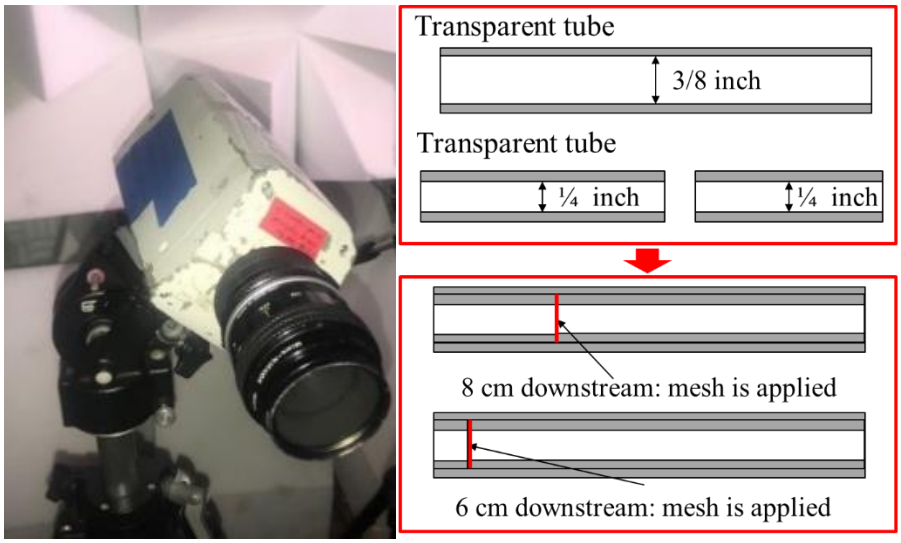

Figure 2. System schematic (a) experimental setup (b) high-speed camera (c) installation of mesh in the transparent tube

4. RESULTS AND DISCUSSION

Figures 3 and 4 show the spectra comparison for the straight and angle valves. After applying the mesh at the outlet, the bubbles generated are broken into smaller ones when passing through the mesh. In this case, the frequency distribution changes after installing the mesh. Since the mesh size is smaller than 0.5mm, the proportion of the high-frequency noise increases according to the spectra, while the proportion of the low-frequency noise decreases. Since the human audible zone is from 20 Hz to 20 kHz, some high-frequency noise generated by the mesh cannot be heard by human beings, so the overall noise level decreases. Figure 5 shows the flow regimes before and after passing through the mesh. It can be seen from the graph that after passing the mesh, the bubbles and droplets break into bubbles and droplets with smaller sizes, and the flow velocity is accelerated by passing through the mesh. The visualization validates that the mesh can control bubbles' size so that the flow-induced noise's frequency distribution changes.

(a) (b)

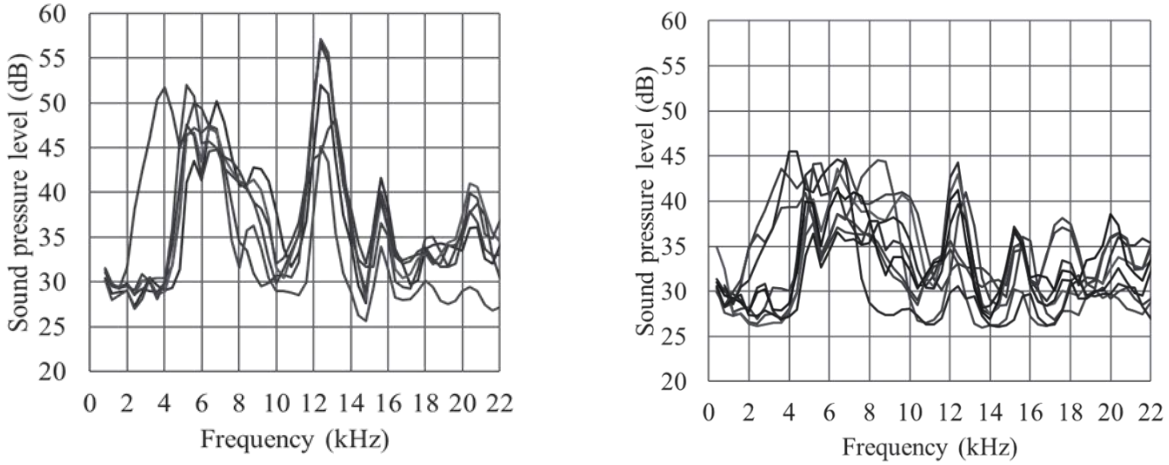

Figure 3. Spectra comparison of flow-induced noise for angle needle valve (a) without stainless steel mesh (b) with stainless steel mesh at the valve outlet

(a) (b)

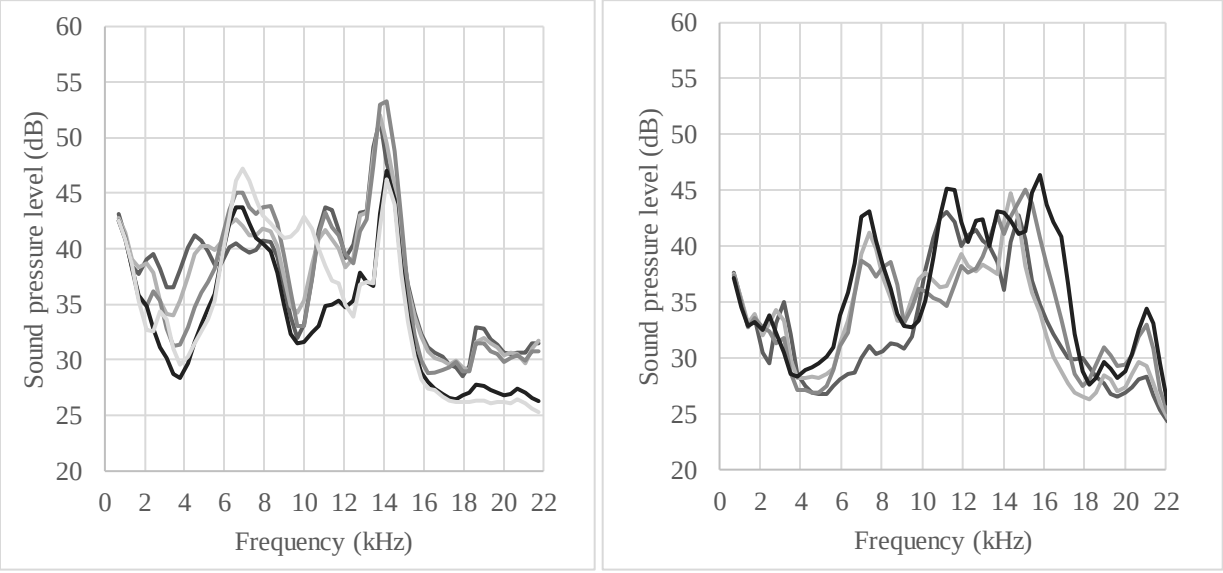

Figure 4. Spectra comparison of flow-induced noise near straight needle valve (a) without stainless steel mesh (b) with stainless steel mesh at the valve outlet

However, Figure 6(a) shows the flow mass flux after passing through the mesh with different sizes. The mesh structure reduces the flow's passing area and therefore increases mass flux. Since that the structure of different mesh sizes varies (i.e., the diameter of the steel line is different for different mesh sizes), the opening area of the mesh for different sizes is not only related to the mesh size. For example, the opening area for the 75-micron mesh is the largest so that the acceleration effect of flow is lowest for the 75-micron mesh. The acceleration effect of mesh is supposed to increase the annoyance of flow-induced noise. Therefore, as a balancing result of accelerating and frequency control effects, the best noise mitigation effect appears when the 75-micron mesh is used, as shown in Figure 6(b).

For one thing, the mesh can break the bubbles into smaller ones that appear at the need valve downstream. The control of frequency distribution decreases the annoyance of flow-induced noise. For another, the acceleration of flow may increase the annoyance of noise. Since the acceleration effect of flow is lowest for the 75-micron mesh, the 75-micron mesh should have the best noise mitigation result. When the mesh size is smaller than 50 microns, the control of frequency distribution is more dominant in noise mitigation. When the mesh size is bigger than 75 microns, the acceleration of flow begins to impact the noise mitigation effect.

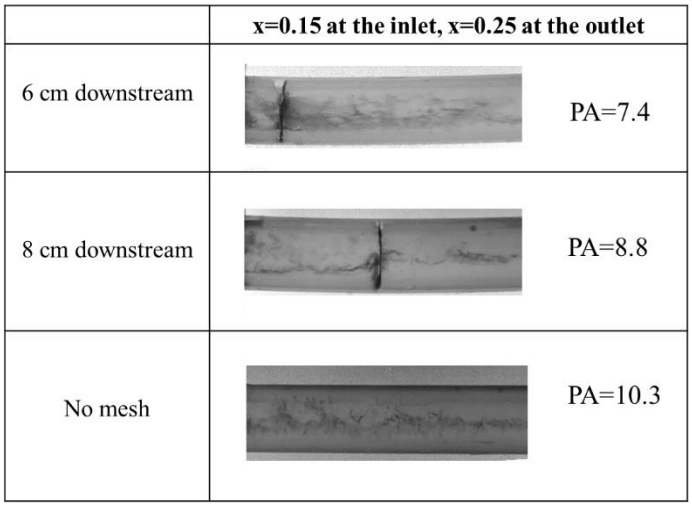

Figure 5. Visualization comparison before and after passing through the mesh

(a) (b)

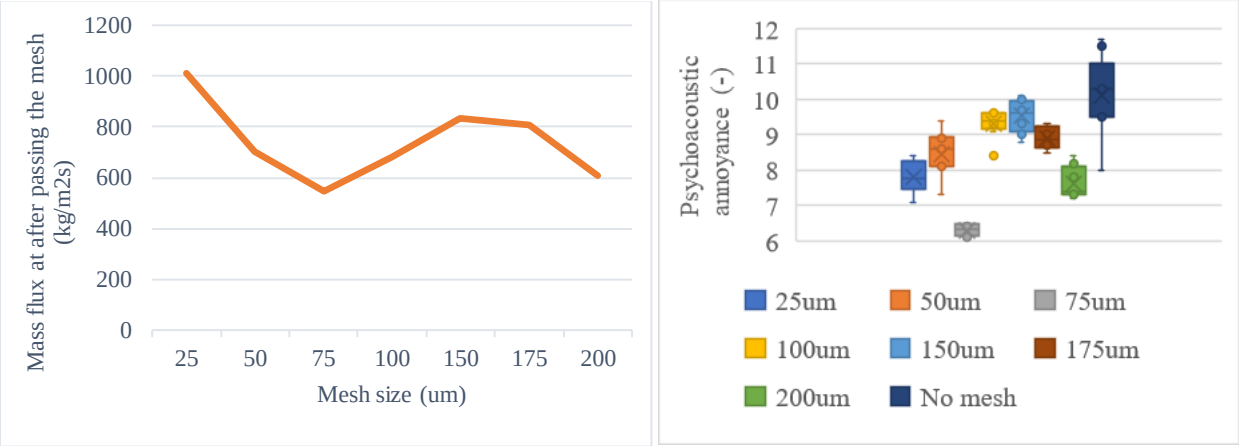

Figure 6. Noise mitigation effect for mesh with different sizes (a) relationship between the mesh size and mass flux after passing through the mesh (b) relationship between the mesh size and the psychoacoustic annoyance

5. CONCLUSIONS

In this paper, a new method for mitigating flow-induced noise is introduced. By installing stainless steel mesh at the valve outlet, the size of bubbles and droplets can be controlled. And the frequency distribution of flow-induced noise can be controlled. As a result, the oscillation frequency of bubbles exceeds the human audible zone so that the annoyance of flow-induced noise decreases. The visualization validates that the mesh can control the size of bubbles and droplets. The mitigation effect is also related to the opening area of the mesh, which increases the annoyance of flow-induced noise. The smaller the opening area is, the higher the mass flux is. The higher mass flux induces more annoying noise than the lower mass flux. It is found in this paper that when the mesh size is 75 microns, the noise mitigation effect is the best.

6. NOMENCLATURE

Symbols:		
g'	weighted coefficient	(-)
f	frequency	(Hz)
L	loudness	(sone)
N'	loudness density	(sone bark^{-1})
P	pressure	(Pa)
PA	psychoacoustic annoyance	(-)
r	radius	(m)
S	sharpness	(acum)
SPL	sound pressure level	(dB)
x	vapor mass fraction (quality)	(-)
k	bark number	(-)
Subscripts:		
l	liquid	
na	natural frequency	
Greek:		
Υ	polytropic exponent	(-)
ρ	density	(kg m^{-3})

REFERENCES

[1] Han, H. S., Jeong, W. B., Kim, M. S., Lee, S. Y., and Seo, M. Y., 2010. Reduction of the refrigerant-induced noise from the evaporator-inlet pipe in a refrigerator. Int J Refrig. , 33(7), 1478–1488.
[2] Wang L., Zhang, G., Wu, H., Yang, J., Zhu, Y., 2016. A top view optical approach for observing the coalescence of liquid droplets. Review of Scientific Instruments, 87(2), 026103.
[3] Kim, G., and Song, S., 2020. Noise reduction of refrigerant two-phase flow using flow conditioners near the electric expansion valve. J. Mech. Sci, 34(2), 719–725.
[4] Minnaert, W.K., 1933. On musical air bubbles and the sound of running water. Philos. Mag., 16(104), 235–248.
[5] Zwicker, E., Fastl, H., 1999. Psychoacoustics: Facts and Models. 2nd edition, Springer-Verlag, New York.

ACKNOWLEDGEMENT

The authors would like to thank the member companies of the Air Conditioning and Refrigeration Center at the University of Illinois at Urbana-Champaign for their financial and technical support and Creative Thermal Solutions, Inc. (CTS) for their technical support. Funding was received through ACRC projects #364 and #416.